

HOREENET: 3D-AWARE HAND-OBJECT GRASPING REENACTMENT

Changhwa Lee^{1,2}, Junuk Cha¹, Hansol Lee¹, Seongyeong Lee^{1,3}, Donguk Kim¹, Seungryul Baek¹

UNIST, South Korea¹, Kakao Brain Corp, South Korea², NC Soft, South Korea³

ABSTRACT

We present HOREeNet, which tackles the novel task of manipulating images involving hands, objects, and their interactions. Especially, we are interested in transferring objects of source images to target images and manipulating 3D hand postures to tightly grasp the transferred objects. Furthermore, the manipulation needs to be reflected in the 2D image space. In our reenactment scenario involving hand-object interactions, 3D reconstruction becomes essential as 3D contact reasoning between hands and objects is required to achieve a tight grasp. At the same time, to obtain high-quality 2D images from 3D space, well-designed 3D-to-2D projection and image refinement are required. Our HOREeNet is the first fully differentiable framework proposed for such a task. On hand-object interaction datasets, we compared our HOREeNet to the conventional image translation algorithms and reenactment algorithm. We demonstrated that our approach could achieved the state-of-the-art on the proposed task.

Index Terms— Image translation, Hand-object interaction

I. INTRODUCTION

Simulating and visualizing interacting hands with diverse tools and objects [1–4] is an important application of virtual reality (VR) and augmented reality (AR). While the simple rendering pipeline of hand and object 3D meshes could achieve the goal; there are few challenges that prevent accomplishing it using commercial 3D rendering pipelines (e.g. Blender, MAYA, ZBrush, etc.): 1) most pipelines work only for objects whose 3D meshes and textures are pre-given; thus types of rendered objects are limited as collecting 3D meshes and textures takes effort, 2) the physical simulator is not involved in the rendering pipelines; while it is essential to simulate the surface contact between hand and object meshes in this scenario, 3) the quality of rendered images frequently have a gap to realistic images. Motivated by the recent success of image manipulation approaches, in this paper, we propose an alternative approach that achieves the scenario of re-enacting hand-object grasps, *hand-object grasping reenactment* that transfers objects of an image to the other image, manipulates hand postures to tightly grasp the transferred object as in Fig. 1. Since we are based on image manipulation, it is possible to involve objects whose 3D meshes and textures are unknown. We also propose the *HOREeNet*, an image synthesis network that learns to re-enact hand-object grasps reflecting the 3D surface contacts and enhancing image qualities.

In our pipeline, we propose to reconstruct both hand and object 3D meshes, manipulate and project them onto the 2D image space via deep learning methods: The entire structure is composed of 4 distinct differentiable modules that 1) estimate 3D meshes of hands and objects from both source and target images, 2) exchange source and target object meshes and manipulate 3D poses of hands to tightly grasp translated objects, 3) project manipulated hand and object meshes into 2D images and refine the quality of projected

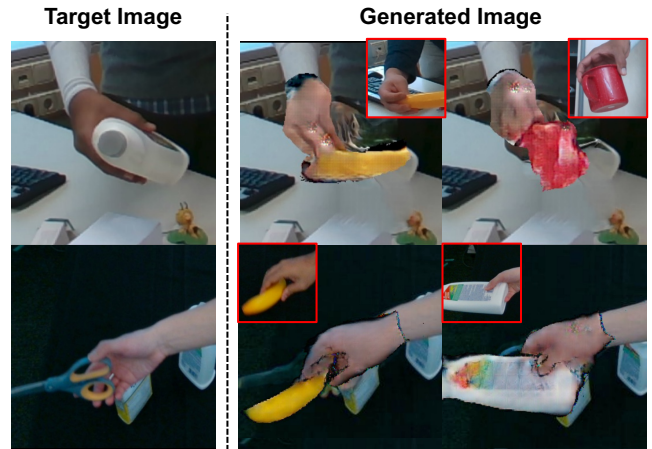


Fig. 1: Given a pair of source (red box) and target images, source \mathbf{x}_{src} 's object is transferred to the target \mathbf{x}_{tar} , hand pose parameters in \mathbf{x}_{tar} are manipulated to tightly grasp the object. Finally, a new image is generated for the new interaction.

2D foreground images. 4) After that, the foreground region of the background image is in-painted and combined with the refined foreground image to generate the final image.

Our contribution in this paper could be summarized as follows:

- We propose to deal with a novel hand-object grasp reenactment task that transfers objects from source to target images, manipulates hand poses of target images for the tight grasp and, generates quality 2D images reflecting 3D manipulation.
- We present HOREeNet, a fully differentiable framework for tackling such a challenging task. The entire system is engineered to achieve the successful hand-object grasping reenactment effectively.
- We perform experiments to prove the superiority of our algorithm over other competitive baselines.

II. RELATED WORKS

Hand pose estimation. Hand pose estimation is proposed to map the single images towards 3D skeletal representation [5,6]. Recently, the end-to-end framework for estimating full 3D meshes from RGB images have been established in [7, 8] using the MANO model [9]. Joint reconstruction of hands and objects was dealt with in [10].

Reenactment. In facial domain, model-based works [11] propose to use facial landmark points to represent the motion (pose and expression). Instead of landmarks, some works [12] tried to use latent features to represent facial identity and motion. [13] proposed the action unit (AU) that aims at modeling the specific muscle activities and insist that each combination of them can produce different

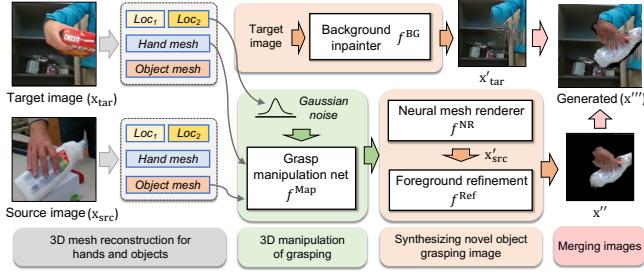


Fig. 2: A schematic diagram of the proposed hand-object interaction reenactment framework: First, hand and object meshes are inferred. Then, the source object and target hand are used to infer the tight hand grasps via the grasp manipulation network f^{Map} . The 2D image x'_{src} is generated via projecting 3D meshes using neural mesh renderer f^{NR} and it is refined towards x'' by the foreground refinement network f^{Ref} to have the realistic quality. At the same time, the original target image x_{tar} is used to generate the background image x'_{tar} by inpainting removed foreground regions (i.e., hands, objects). Finally, x''' is generated by merging x'' and x'_{tar} .

facial expression, which allows editing without identity distortion. In human body domain, clothing reenactment is proposed to transfer a target clothing item onto the corresponding region of a human body [14]. There have been a work to estimate clothing deformations to the target body [15]. [16] proposed a method that infers 3D body structures and manipulates it through geometric warping.

Image-to-image translation. Image translation has gained considerable attention generative adversarial networks (GANs) [17, 18]. Though the GAN method is originally derived for the unsupervised setting, the supervised learning method for GANs that conditions the latent space on the label space was suggested in [19].

III. PIPELINE

Our aim here is to achieve the *hand-object grasp reenactment* task that exchanges objects of source and target images, learn to find proper hand grasps for the exchanged object, and generates quality 2D images. Towards that direction, we defined 4 steps in our pipeline as in Fig. 2, which are detailed in Sec. 3.1 through Sec. 3.4.

3.1. 3D mesh reconstruction for hands and objects

We first proposed to estimate 3D meshes of hands and objects (i.e. $\mathbf{m} = \{\mathbf{m}_H, \mathbf{m}_O\}$), location parameters for hand meshes (i.e., c_1, c_2) given an RGB image \mathbf{x} (cf. we used two types of location parameters, $\mathbf{c} = [c_1, c_2]$, which are used to transform the mesh within the original MANO [9] space and transform the mesh from MANO space to the image space, respectively). Additionally, to infer textures of hand and object meshes, we involved the texture inference network f^{Tex} , which infers RGB texture vector \mathbf{t} corresponding to faces of the 3D meshes $\mathbf{m} = \{\mathbf{m}_H, \mathbf{m}_O\}$.

Hand mesh reconstruction network f^{Hand} . The hand mesh reconstruction network $f^{\text{Hand}} : \mathbf{x} \rightarrow [\mathbf{m}_H(\theta, \beta), \mathbf{c}]$ is defined to input the 2D image \mathbf{x} and output the location parameters $\mathbf{c} = [c_1, c_2]$ and 3D hand mesh $\mathbf{m}_H(\theta, \beta) \in \mathbb{R}^{778 \times 1,538}$. The 3D hand mesh $\mathbf{m}_H(\theta, \beta)$ is parameterized by θ and β , which denotes pose and shape parameters of the MANO model, respectively [9]. Both location parameters c_1 and c_2 have seven scalar values: 1 for scale, 2 for x and y translation, and 4 for quaternion, respectively. We employed the architecture of the convolutional pose machine (CPM) [20] combined with

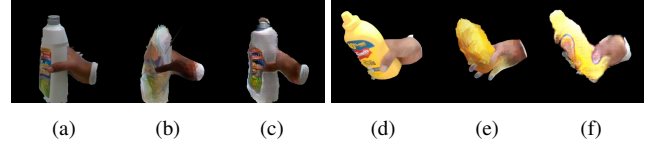


Fig. 3: Ablation study for with and without the use of the foreground refinement network f^{Ref} . (a, d) Ground-truth image, (b, e) Generated image before f^{Ref} , (c, f) Refined image after f^{Ref} .

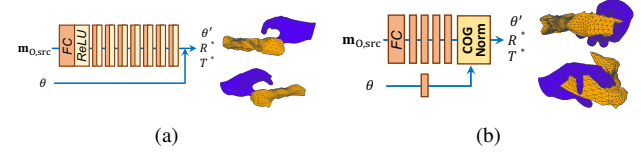


Fig. 4: Ablation study on the use of COG-Norm layer. (a) the parameter size of the grasp manipulation network f^{Map} having only MLP layers is 0.97M; (b) the parameter size of the grasp manipulation network f^{Map} with COG-Norm layer is 0.49M. Also, we can observe that in (b), reconstructed hand-object meshes are more tightly aligned compared to the one in (a).

the MANO layer [9] to first estimate 2D heatmaps of the hands and then estimate the 3D hand meshes upon it.

Object mesh reconstruction network f^{Object} . Our 3D object mesh reconstruction network $f^{\text{Object}} : \mathbf{x} \rightarrow \mathbf{m}_O \in \mathbb{R}^{2,466 \times 4,928}$ used the same architecture as Pixel2Mesh [21].

Texture inference network f^{Tex} . Our texture inference network $f^{\text{Tex}} : \mathbf{x} \rightarrow \mathbf{t} \in \mathbb{R}^{N_f \times T \times T \times T \times 3}$ uses the ResNet-50 architecture to infer the RGB texture vector \mathbf{t} that corresponds to each face of 3D meshes \mathbf{m} . T is the minimum dimension for \mathbf{t} and it is set to 2.

3.2. 3D manipulation of novel hand grasping

To adjust hand postures of the target image x_{tar} to tightly grasp the translated 3D object meshes $\mathbf{m}_{O,\text{src}}$ of the source image x_{src} , we proposed a grasp manipulation network f^{Map} that manipulates the pose parameter θ of the initial hand mesh $\mathbf{m}_{H,\text{tar}}$. We propose the **COntact-aware Grasp Normalization (COG-Norm)** layer to effectively output a new hand pose parameter θ' for $\mathbf{m}_{H,\text{tar}}$ by mixing vertice information of predicted hands and objects.

Grasp manipulation network f^{Map} . In the COG-Norm layer, the pose parameter is normalized and modulated with the features of $\mathbf{m}_{O,\text{src}}$ obtained by the function γ and α , which are composed of fully-connected layers. The activation formulation is calculated as below ($i \in [1, 45]$):

$$\begin{aligned} \text{COG-Norm}(\theta_i, \mathbf{m}_{O,\text{src}}) &= \gamma(\mathbf{m}_{O,\text{src}}) \frac{\theta_i - \mu(\theta)}{\sigma(\theta)} \\ &+ \alpha(\mathbf{m}_{O,\text{src}}) \end{aligned} \quad (1)$$

where θ_i , μ and σ are the i -th element of the θ , the mean and standard deviation of MANO pose parameters.

3.3. Synthesizing novel object grasping image

Neural 3D mesh renderer f^{NR} . Neural 3D mesh renderer $f^{\text{NR}} : [\mathbf{m}, \mathbf{t}, c_2] \rightarrow x'$ is used to render the reconstructed 3D meshes \mathbf{m} and its texture vector \mathbf{t} to the 2D image x' . We employ the implementation of [22] for this.

Foreground refinement network f^{Ref} . We proposed to employ the foreground refinement network $f^{\text{Ref}}: \mathbf{x}' \rightarrow \mathbf{x}''$ to refine the initial 2D images \mathbf{x}' towards more realistic 2D images \mathbf{x}'' . Its architecture is same as the generation network of [23].

Background in-painter f^{BG} . Background in-painter is used to reuse the background of the target image \mathbf{x}_{tar} . We propose to remove the foreground objects in the target image \mathbf{x}_{tar} using the inpainting algorithm: 1) we re-projected the estimated hand and object 3D meshes \mathbf{m} to generate the 2D foreground mask \mathbf{s}_{tar} having binary values (1 for foreground objects, 0 for backgrounds), 2) then we applied the in-painting network of [24] pre-trained on Places2 [25] dataset onto $(1 - \mathbf{s}_{\text{tar}}) \odot \mathbf{x}_{\text{tar}}$ to obtain the in-painted image \mathbf{x}'_{tar} .

3.4. Merging images.

The final image \mathbf{x}''' is generated by merging the refined image \mathbf{x}'' and background-inpainted image \mathbf{x}'_{tar} using the foreground mask \mathbf{s} rendered from hand and object meshes $[\mathbf{m}_{\text{H,tar}}(\theta'), \mathbf{m}_{\text{O,src}}]$:

$$\mathbf{x}''' = \mathbf{x}'' \odot \mathbf{s} + \mathbf{x}'_{\text{tar}} \odot (1 - \mathbf{s}) \quad (2)$$

where \odot denotes the element-wise multiplication operation.

Aligning wrist positions. When aligning arms in the target image \mathbf{x}_{tar} with the transferred hand postures, we choose the 1 wrist point of the hand mesh \mathbf{m}_{H} that is estimated from \mathbf{x}_{tar} . Then, we translate the absolute position of the transferred hand and object meshes by making its wrist point coincide with the kept wrist point.

IV. TRAINING METHOD

Our training method is composed of two steps: 1) a step for training $f^{\text{Hand}}, f^{\text{Object}}, f^{\text{Tex}}, f^{\text{Ref}}$ and 2) a step for training f^{Map} . At the first step, we use the loss function \mathcal{L}_{HO} to train four networks: $f^{\text{Hand}}, f^{\text{Object}}, f^{\text{Tex}}, f^{\text{Ref}}$:

$$\begin{aligned} \mathcal{L}_{\text{HO}}(f^{\text{Hand}}, f^{\text{Object}}, f^{\text{Tex}}, f^{\text{Ref}}) &= \mathcal{L}_{\text{Hand}}(f^{\text{Hand}}) \\ &+ \lambda_{\text{ho},1} \mathcal{L}_{\text{Object}}(f^{\text{Object}}) + \lambda_{\text{ho},2} \mathcal{L}_{\text{Tex}}(f^{\text{Tex}}) + \lambda_{\text{ho},3} \mathcal{L}_{\text{Ref}}(f^{\text{Ref}}) \end{aligned}$$

where $\lambda_{\text{ho},1} = 1$, $\lambda_{\text{ho},2} = 0.01$, and $\lambda_{\text{ho},3} = 0.1$ are used to balance each term. Then, we train the f^{Map} using the loss \mathcal{L}_{Map} in Eq. 9. The first step is executed for 30 epochs and the second step is processed for 15 epochs. We trained the entire network using the Adam optimizer with $\beta = (0.5, 0.999)$ and a learning rate of 10^{-4} for hand and object reconstruction networks: $f^{\text{Hand}}, f^{\text{Object}}$ while 10^{-5} for all others. Each loss term is detailed in the remainder of this section:

Hand mesh estimation loss $\mathcal{L}_{\text{Hand}}$. This loss is used to train the hand mesh reconstruction network f^{Hand} by 1) closing hand meshes \mathbf{m}_{H} to its ground-truths $\mathbf{m}_{\text{H,GT}}$ and, 2) closing 3D skeletons $J(\mathbf{m}_{\text{H}})$ and 2D skeletons $\psi_{\mathbf{c}_2}(J(\mathbf{m}_{\text{H}}))$ regressed from hand meshes to their ground-truths \mathbf{j}_{GT} and $\mathbf{j}_{2\text{DGT}}$, respectively:

$$\begin{aligned} \mathcal{L}_{\text{Hand}}(f^{\text{Hand}}) &= \|\psi_{\mathbf{c}_1}(\mathbf{m}_{\text{H}}) - \psi_{\mathbf{c}_1}(\mathbf{m}_{\text{H,GT}})\|_1 \\ &+ \|\psi_{\mathbf{c}_1}(J(\mathbf{m}_{\text{H}})) - \mathbf{j}_{\text{GT}}\|_2^2 + \|\psi_{\mathbf{c}_2}(J(\mathbf{m}_{\text{H}})) - \mathbf{j}_{2\text{DGT}}\|_2^2 \quad (3) \end{aligned}$$

where the projection function $\psi_{\mathbf{c}}$ applies scale, translation, and rotation transformations to 3D meshes using \mathbf{c} . The network $J(\cdot)$ provided by [9] geometrically regresses 3D skeletons \mathbf{j} from mesh \mathbf{m}_{H} .

Object mesh estimation loss $\mathcal{L}_{\text{Object}}$. This loss is defined as follows:

$$\mathcal{L}_{\text{Object}}(f^{\text{Object}}) = L_{\text{chamfer}}(f^{\text{Object}}) + L_{\text{edge}}(f^{\text{Object}}) + L_{\text{lap}}(f^{\text{Object}}) \quad (4)$$

where chamfer loss $L_{\text{chamfer}} = \sum_p \min_q \|p - q\|_2^2 + \sum_q \min_p \|p - q\|_2^2$, edge loss $L_{\text{edge}} = \sum_p \sum_{k \in N(p)} \|p - k\|_2^2$, and Laplacian loss

$L_{\text{lap}} = \sum_p \|\delta'_p - \delta_p\|_2^2$ are employed from [21] to train the 3D object mesh reconstruction network.

Texture inference loss \mathcal{L}_{Tex} . This loss is used to train the texture inference network f^{Tex} by making the rendered RGB images from hand-object meshes with the inferred textures $f^{\text{Tex}}(\mathbf{x})$ same as the segmented foreground regions of the original image \mathbf{x} :

$$\mathcal{L}_{\text{Tex}}(f^{\text{Tex}}) = \|f^{\text{NR}}([\mathbf{m}_{\text{H}}, \mathbf{m}_{\text{O}}], f^{\text{Tex}}(\mathbf{x}), \mathbf{c}_2) - \mathbf{x} \odot \mathbf{s}'\|_2^2 \quad (5)$$

where \mathbf{s}' is a foreground mask rendered from meshes $\mathbf{m} = [\mathbf{m}_{\text{H}}, \mathbf{m}_{\text{O}}]$.

Refinement loss \mathcal{L}_{Ref} . This loss is used to train the foreground refinement network f^{Ref} to generate more realistic images $\mathbf{x}'' = f^{\text{Ref}}(\mathbf{x}')$ from \mathbf{x}' .

$$\mathcal{L}_{\text{Ref}}(f^{\text{Ref}}) = L_{\text{GAN}}(f^{\text{Ref}}) + L_P(f^{\text{Ref}}) \quad (6)$$

where

$$\begin{aligned} L_{\text{GAN}}(f^{\text{Ref}}) &= \mathbb{E}_{(\mathbf{x}', \mathbf{x})} [\log D^{\text{Ref}}(\mathbf{x}', \mathbf{x})] \\ &+ \mathbb{E}_{\mathbf{x}'} [\log(1 - D^{\text{Ref}}(\mathbf{x}', f^{\text{Ref}}(\mathbf{x}')))], \quad (7) \end{aligned}$$

$$L_P(f^{\text{Ref}}) = \sum_{i=1}^N \frac{1}{M_i} [\|F^{(i)}(\mathbf{x}) - F^{(i)}(f^{\text{Ref}}(\mathbf{x}'))\|_1] \quad (8)$$

where D^{Ref} is the GAN-type discriminator network [17] and $F^{(i)}$ denotes the i -th layer of the VGG-19 network having M_i elements which is involved to capture the perceptual characteristics [29].

Grasp manipulation loss \mathcal{L}_{Map} . This loss is used to train the grasp manipulation network f^{Map} that learns to control the hand postures to grasp the objects tightly:

$$\mathcal{L}_{\text{Map}}(f^{\text{Map}}) = L_{\text{contact}}(f^{\text{Map}}) + L_{\text{cent}}(f^{\text{Map}}) + L_{\text{adv}}(f^{\text{Map}}) \quad (9)$$

where

$$L_{\text{contact}}(f^{\text{Map}}) = \frac{1}{|\mathbf{v}_{\text{contact}}|} \sum_{v \in \mathbf{v}_{\text{contact}}} \min_k \|v, \mathbf{m}_{\text{O}}^k\|_2 \quad (10)$$

$$L_{\text{cent}}(f^{\text{Map}}) = \frac{1}{2} \|\mathbb{C}(\mathbf{m}_{\text{O}}) - \mathbb{C}(\mathbf{m}_{\text{H}})\|_2^2 \quad (11)$$

$$\begin{aligned} L_{\text{adv}}(f^{\text{Map}}) &= -\mathbb{E}_{\theta} [D(\theta)] + \mathbb{E}_{\theta_{\text{GT}}} [D(\theta_{\text{GT}})] \\ &+ \lambda \mathbb{E}_{\theta} [(\|\nabla_{\theta} D(\theta)\|_2 - 1)^2] \quad (12) \end{aligned}$$

where contact loss L_{contact} is used to minimize the distance between 3D object vertices \mathbf{m}_{O}^k and pre-defined vertices of hands $\mathbf{v}_{\text{contact}}$ that are frequently involved for the grasping, centroid loss L_{cent} is used to minimize the center position of hand and objects where $\mathbb{C}(\cdot)$ denotes the centroid of 3D meshes and the adversarial loss L_{adv} is involved to constitute the adversarial [17] and Wasserstein [30] losses via the discriminator D , respectively. Via L_{contact} and L_{centroid} , f^{Map} is learned to obtain the tight 3D grasp between objects and hand meshes. Also, L_{adv} enforces f^{Map} to obtain the hand grasps within the realistic grasping distribution.

V. EXPERIMENT

Dataset. We conducted our experiments on two types of datasets: Honnotate [26] and DexYCB [27]. For Honnotate dataset, we used the entire dataset, while for DexYCB dataset, we used the default split: sub-sampling ten out of twenty subjects, one out of eight views excluding non-grasping frames when constituting the dataset.

Results. We involved two conventional image translation methods (i.e., CycleGAN [17] and U-GAT-IT [18]) with one face reenactment

Table 1: Quantitative results comparing ours to three state-of-the-art image translation methods (i.e., CycleGAN [17], U-GAT-IT [18], and ReenactGAN [12]) on Honnotate [26] and DexYCB [27] datasets. The evaluation is performed using three measures: FID [28], LPIPS [29] based on AlexNet, and LPIPS based on VGG. For all measures, lower is better and best results are bold-faced.

DB Stream Model	Honnotate [26]			DexYCB [27]		
	A → B	A → C	B → C	A → B	A → C	B → C
	B → A	C → A	C → B	B → A	C → A	C → B
CycleGAN	914.4 / 0.478 / 0.583	843.2 / 0.546 / 0.611	915.6 / 0.583 / 0.661	509.8 / 0.227 / 0.361	497.0 / 0.244 / 0.353	627.0 / 0.180 / 0.277
	887.8 / 0.575 / 0.632	839.2 / 0.584 / 0.637	984.9 / 0.590 / 0.608	758.6 / 0.255 / 0.377	502.4 / 0.179 / 0.290	612.3 / 0.208 / 0.343
U-GAT-IT	734.2 / 0.443 / 0.533	788.1 / 0.624 / 0.689	864.0 / 0.612 / 0.696	502.0 / 0.269 / 0.411	496.3 / 0.285 / 0.430	490.0 / 0.211 / 0.347
	781.8 / 0.526 / 0.631	872.0 / 0.630 / 0.693	1011.3 / 0.640 / 0.688	561.5 / 0.252 / 0.387	477.0 / 0.261 / 0.400	519.0 / 0.251 / 0.406
ReenactGAN	1845.7 / 0.482 / 0.466	1491.1 / 0.440 / 0.381	1707.1 / 0.372 / 0.376	1102.9 / 0.484 / 0.473	1268.3 / 0.519 / 0.496	1313.0 / 0.521 / 0.472
	1530.8 / 0.370 / 0.415	1470.6 / 0.372 / 0.414	1732.6 / 0.364 / 0.422	1806.3 / 0.500 / 0.454	1917.0 / 0.532 / 0.454	1447.8 / 0.512 / 0.467
Ours	862.9 / 0.713 / 0.541	828.9 / 0.674 / 0.528	997.7 / 0.771 / 0.618	443.0 / 0.227 / 0.210	483.7 / 0.153 / 0.212	558.2 / 0.151 / 0.207
(w/o f^{Ref})	983.1 / 0.768 / 0.617	917.6 / 0.634 / 0.565	939.3 / 0.637 / 0.573	585.9 / 0.154 / 0.214	545.3 / 0.249 / 0.304	536.5 / 0.258 / 0.316
Ours	777.6 / 0.417 / 0.397	752.7 / 0.383 / 0.368	636.9 / 0.184 / 0.180	404.1 / 0.132 / 0.197	399.0 / 0.130 / 0.197	522.2 / 0.144 / 0.192
	585.6 / 0.168 / 0.167	851.9 / 0.242 / 0.248	891.7 / 0.285 / 0.286	525.1 / 0.138 / 0.191	517.1 / 0.176 / 0.218	542.3 / 0.177 / 0.223

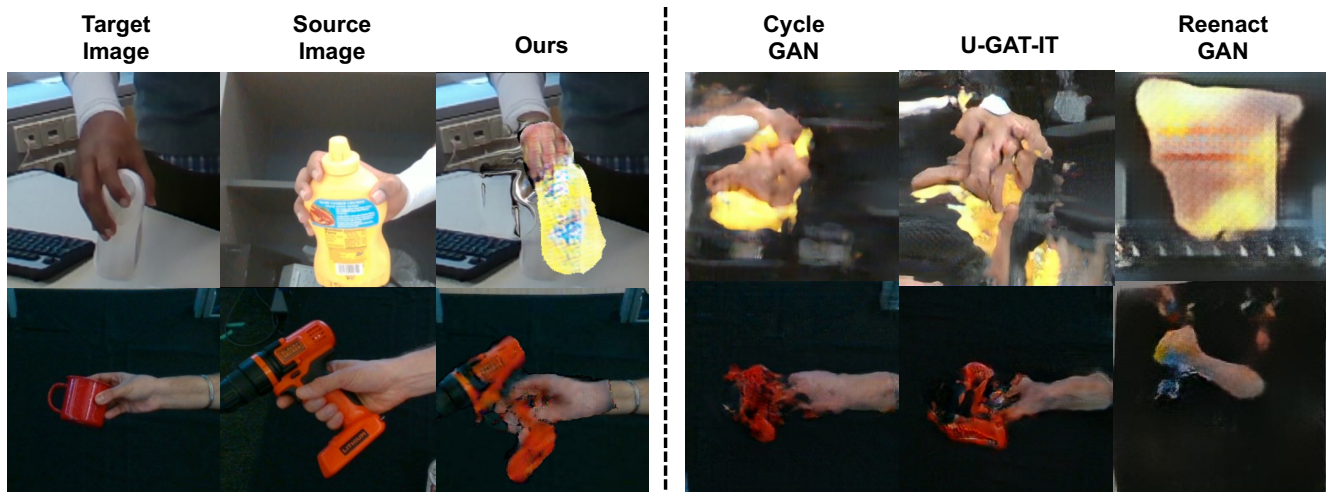


Fig. 5: Examples from Ours and other baselines (CycleGAN, U-GAT-IT and ReenactGAN) on Honnotate [26] (first rows) and DexYCB [27] (last rows). Ours faithfully generates 2D images; while others show incomplete results.

method (i.e., ReenactGAN [12]) to compare with our method. We found that ours obtained the superior performance in three measures (i.e., FID [28], LPIPS [29] based on AlexNet and LPIPS based on VGG) compared to three algorithms as shown in Table 1. For the binary domain transfer, we picked three objects as domains: (A) potted meat can, (B) bleach cleanser, and (C) mustard bottle and trained the model for the bi-directional transfer (i.e., $A \rightarrow B$, $B \rightarrow A$, $A \rightarrow C$, $C \rightarrow A$, $B \rightarrow C$, and $C \rightarrow B$).

Fig. 5 shows the qualitative examples for two datasets. We visualize the results from 2D image translation methods (ie. CycleGAN [17], U-GAT-IT [18]), denoting that the 2D image manipulation models are not able to understand the foreground objects. We also compared ours with reenactment algorithm (ie. ReenactGAN [12]) as well; however it fails to deliver the reenactment of hand-object grasping, even though it exploits 2D poses of the foreground objects. On the contrary, ours faithfully maintain the background of target images while changing only foreground pixels.

Ablation study. We additionally conducted ablation studies for our foreground refinement network f^{Ref} and COG-Norm layer proposed in the grasp manipulation network f^{Map} . In Fig. 3 and Table. 1, we

showed the results with and without the foreground refinement network f^{Ref} . The result is quantitatively and qualitatively better when f^{Ref} is involved. In Fig. 4, we attached qualitative results comparing the grasp manipulation network f^{Map} constructed using only FC layers versus the one using the proposed COG-Norm layer. From this, we could find that the use of the COG-Norm layer makes a huge difference: it makes the entire grasp manipulation network f^{Map} work better and faster than before.

VI. CONCLUSION

We have introduced the novel scenario of hand-object grasp reenactment and the HOReeNet, a fully differentiable pipeline that is able to deal with the scenario. It performs better than conventional image translation and face reenactment algorithms on the novel task. From ablative experiments, we also observed that proposed sub-modules operate in the meaningful way. We expect the proposed method and scenario could be the stepping stone for future research that offers 3D information in 2D-based generative networks.

VII. REFERENCES

- [1] Bailin Li, Yaxiong Bi, Qiang He, Jie Ren, and Zhaohui Li, “A low-complexity method for authoring an interactive virtual maintenance training system of hydroelectric generating equipment,” *Computers in Industry*, 2018.
- [2] George D. Lecakes, Michael Russell, Shreekanth Mandayam, Jonathan A. Morris, and John L. Schmalzel, “Visualization of multiple sensor measurements in a vr environment for integrated systems health management in rocket engine tests,” *IEEE Sensors Applications Symposium*, 2009.
- [3] Chul Gyu Song, Jong Yun Kim, and Nam Gyun Kim, “A new postural balance control system for rehabilitation training based on virtual cycling,” *IEEE Transactions*, 2004.
- [4] Shangchen Han, Beibei Liu, Robert Wang, Yuting Ye, Christopher D. Twigg, and KenrickKi Kin, “Online optical marker-based hand tracking with deep labels,” *ACM Trans. Graph.*, 2018.
- [5] Christian Zimmermann and Thomas Brox, “Learning to estimate 3d hand pose from single rgb images,” in *ICCV*, 2017.
- [6] Seungryul Baek, Kwang In Kim, and Tae-Kyun Kim, “Augmented skeleton space transfer for depth-based hand pose estimation,” in *CVPR*, 2018.
- [7] Seungryul Baek, Kwang In Kim, and Tae-Kyun Kim, “Pushing the envelope for rgb-based dense 3d hand pose estimation via neural rendering,” in *CVPR*, 2019.
- [8] Seungryul Baek, Kwang In Kim, and Tae-Kyun Kim, “Weakly-supervised domain adaptation via gan and mesh model for estimating 3d hand poses interacting objects,” in *CVPR*, 2020.
- [9] Javier Romero, Dimitrios Tzionas, and Michael J. Black, “Embodied hands: Modeling and capturing hands and bodies together,” *ToG*, 2017.
- [10] Yana Hasson, Gul Varol, Dimitrios Tzionas, Igor Kalevatykh, Michael J Black, Ivan Laptev, and Cordelia Schmid, “Learning joint reconstruction of hands and manipulated objects,” in *CVPR*, 2019.
- [11] Jiangning Zhang, Xianfang Zeng, Mengmeng Wang, Yusu Pan, Liang Liu, Yong Liu, Yu Ding, and Changjie Fan, “Freenet: Multi-identity face reenactment,” in *CVPR*, 2020.
- [12] Wayne Wu, Yunxuan Zhang, Cheng Li, Chen Qian, and Chen Change Loy, “Reenactgan: Learning to reenact faces via boundary transfer,” in *ECCV*, 2018.
- [13] Soumya Tripathy, Juho Kannala, and Esa Rahtu, “Icface: Interpretable and controllable face reenactment using gans,” in *WACV*, 2020.
- [14] Bochao Wang, Huabin Zheng, Xiaodan Liang, Yimin Chen, Liang Lin, and Meng Yang, “Toward characteristic-preserving image-based virtual try-on network,” in *ECCV*, 2018.
- [15] Chaitanya Patel, Zhouyingcheng Liao, and Gerard Pons-Moll, “Tailornet: Predicting clothing in 3d as a function of human pose, shape and garment style,” in *CVPR*, 2020.
- [16] István Sáráncsi Knoche, Markus and Bastian Leibe., “Reposing humans by warping 3d features,” in *CVPR*, 2020.
- [17] Jun-Yan Zhu, Taesung Park, Phillip Isola, and Alexei A Efros, “Unpaired image-to-image translation using cycle-consistent adversarial networks,” in *ICCV*, 2017.
- [18] Kim Junho, Kim Minjae, Kang Hyeonwoo, and Lee Kwanghee, “U-GAT-IT: unsupervised generative attentional networks with adaptive layer-instance normalization for image-to-image translation,” in *ICLR*, 2020.
- [19] Jun-Yan Zhu, Taesung Park, Phillip Isola, and Alexei A Efros, “Unpaired image-to-image translation using cycle-consistent adversarial networks,” in *CVPR*, 2017.
- [20] Shih-En Wei, Varun Ramakrishna, Takeo Kanade, and Yaser Sheikh, “Convolutional pose machines,” in *CVPR*, 2016.
- [21] Nanyang Wang, Yinda Zhang, Zhuwen Li, Yanwei Fu, Wei Liu, and Yu-Gang Jiang, “Pixel2mesh: Generating 3d mesh models from single rgb images,” in *ECCV*, 2018.
- [22] Hiroharu Kato, Yoshitaka Ushiku, and Tatsuya Harada, “Neural 3d mesh renderer,” in *CVPR*, 2018.
- [23] Ting-Chun Wang, Ming-Yu Liu, Jun-Yan Zhu, Andrew Tao, Jan Kautz, and Bryan Catanzaro, “High-resolution image synthesis and semantic manipulation with conditional gans,” in *CVPR*, 2018.
- [24] Zili Yi, Qiang Tang, Shekoofeh Azizi, Daesik Jang, and Zhan Xu, “Contextual residual aggregation for ultra high-resolution image inpainting,” in *CVPR*, 2020.
- [25] Bolei Zhou, Agata Lapedriza, Aditya Khosla, Aude Oliva, and Antonio Torralba, “Places: A 10 million image database for scene recognition,” *IEEE Transactions on Pattern Analysis and Machine Intelligence*, 2017.
- [26] Shreyas Hampali, Mahdi Rad, Markus Oberweger, and Vincent Lepetit, “HONotate: A method for 3D annotation of hand and object poses,” in *CVPR*, 2020.
- [27] Yu-Wei Chao, Wei Yang, Yu Xiang, Pavlo Molchanov, Ankur Handa, Jonathan Tremblay, Yashraj S. Narang, Karl Van Wyk, Umar Iqbal, Stan Birchfield, Jan Kautz, and Dieter Fox, “DexYCB: A benchmark for capturing hand grasping of objects,” in *CVPR*, 2021.
- [28] Martin Heusel, Hubert Ramsauer, Thomas Unterthiner, Bernhard Nessler, and Sepp Hochreiter, “Gans trained by a two time-scale update rule converge to a local nash equilibrium,” in *NIPS*, 2017.
- [29] Richard Zhang, Phillip Isola, Alexei A. Efros, Eli Shechtman, and Oliver Wang, “The unreasonable effectiveness of deep features as a perceptual metric,” in *CVPR*, 2018.
- [30] Ishaan Gulrajani, Faruk Ahmed, Martin Arjovsky, Vincent Dumoulin, and Aaron C Courville, “Improved training of wasserstein gans,” in *NIPS*, 2017.